BJRS
BRAZILIAN JOURNAL OF RADIATION SCIENCES

doi.org/10.15392/2319-0612.2024.2336
2024, 12(1) | 01-19 | e2336
Submitted: 2023-09-06
Accepted: 2023-12-19

Instrumental Neutron Activation Analysis (INAA) Assessment of REE of Soil from Mining Site Umuahia, Abia State, South East, Nigeria

Onudibia[a,b], M. E.; Silva[b], P. S. C.; Essiett[c], A. A.; Zahn[b], G. S.; Genezini[b], F. A.; Linhares[b], H. M. S. M. D.; Nnamani[e], N. C.; Bede[d], M. C; Okoh[a], F.O.; Imeh[c], E. E.; Odoh[a], C. M.

[a] Department of Pure and Applied Physics, Federal University Wukari, Taraba State P.M.B 1020 Kasinala Road, Wukari, Taraba State, Nigeria.

[b] Institute for Energy and Nuclear Research (IPEN), Research Reactor Center (CRPq), University of Sao Paulo (USP), São Paulo, Brazil.

[c] Department of Physics, University of Uyo, Uyo, Akwa-Ibom, Nigeria.

[d] Federal University of Technology, Ikot Abasi, Akwa Ibom State, Nigeria.

[e] Department of Statistics, Ahmadu Bello University, Zaria, Kaduna, Nigeria.

*Correspondence: mosesmarke@gmail.com; m.onudibia@fuwukari.edu.ng

Abstract: In this work, the main goal was to examine the REE concentration and distribution pattern in soil from Umuahia, Abia State, Southeast, Nigeria, in a clay mining site compared with a non-contaminated site approximately 3 km away. The REE were determined by Instrumental Neutron Activation Analysis (INAA) at IPEN, Brazil. The main mineralogy of the samples was determined by XRD. The following REE were determined: Ce, Eu, La, Lu, Nd, Sm, Tb and Yb. Soil samples from the mining area present quartz and kaolinite as their main constituents, with REE concentrations comparable with that of the Upper Continental Crust and the North American Shale Composite. The calculated Geoaccumulation index (IGeo) indicate that REE have natural origin and $\sum LREE_N/\sum HREE_N$ ratio show an enrichment of the light over heavy REE, in samples of the clay mining area.

Keywords: rare earth elements, clay mining soil, Umuahia, Nigeria, geoaccumulation.

BJRS
BRAZILIAN JOURNAL OF RADIATION SCIENCES

doi.org/10.15392/2319-0612.2024.2336
2024, 12(1) | 01-19 | e2336
Submitted: 2023-09-06
Accepted: 2023-12-19

Avaliação de ETR no Solo em Área de Mineração de Umuahia, Estado de Abia, Sudeste da Nigéria por Análise por Ativação Neutrônica Instrumental (INAA)

Resumo: Neste trabalho, o objetivo principal foi examinar a concentração e o padrão de distribuição de elementos terras raras (ETR) no solo de Umuahia, Estado de Abia, do Sudeste da Nigéria, num local de mineração de argila em comparação com um local não contaminado a aproximadamente 3 km de distância. Os ETR foram determinados por Análise por ativação neutrônica instrumental (INAA) no IPEN, Brasil. A mineralogia principal das amostras foi determinada por difração de raios-X. Foram determinados os seguintes ETR: Ce, Eu, La, Lu, Nd, Sm, Tb e Yb. As amostras de solo da área de mineração apresentam quartzo e caulinita como principais constituintes, com concentrações de ETR comparáveis às da crosta continental superior e do composto de xisto norte-americano. O índice de geoacumulação calculado (IGeo) indica que os ETR têm origem natural e a relação ∑LETR/∑PETR mostra um enriquecimento dos ETR leves em relação aos pesados, em amostras da área de mineração de argila.

Palavras-chave: elementos de terras raras, solo de mineração de argila, Umuahia, Nigéria, geoacumulação.

SBPR

1. INTRODUCTION

Soil is the basic and needful part of the earth's crust, the natural medium for the growing of earth's crops and plants, having lots of purposes and uses in everyday activities [1]. Soil is also the host of mineral ores, among them, those containing rare earth elements (REE) [2].

Rare earth elements are the members of fifteen metallic elements that compose the lanthanide series. Some authors include scandium and yttrium in this group [3]. REE have resembling electronic structures providing them similar chemical and physical properties [4], they are also called technology elements or metals because of their wider application in the world of technology as well as in pure science and medicine [5]. There are more than 160 minerals containing these elements, most of them are in the form of silicates, carbonates, oxides and phosphates [6, 7]. The estimated average concentration of the REE in the Earth's crust ranges from around 130 $\mu g\ g^{-1}$ to 240 $\mu g\ g^{-1}$ which is significantly higher than other commonly exploited elements [8]. In trace amounts these elements may be found, besides soil, in plants, water, and the atmosphere. They can also be spread in environments due to anthropogenic activities and be incorporated into the human body through several exposure pathways specifically via food ingestion [9]. The process of discarding old fashioned devices containing REE, applications of phosphate fertilizers containing REE, mining, and scattering/spreads from indigenous rocks may increase the probability of environmental REE contamination [5, 10].

The possible impacts of REE on ecosystems are relatively unknown, therefore, the propensity for exposure and transfer into living organisms needs to be assessed to understand ecosystems and human health threats since the escalation of soil contamination may be continuously increasing because of the input from various human activities such as

mining, industry, agriculture, highways, and road development [11]. Besides that, soil contamination can also originate from geogenic processes such as landslides, terrestrial run-offs, and land erosion [10].

Rare earth elements are classified as: light rare earth elements (LREE) comprising the group formed by La, Ce, Pr, Nd, Sm, Eu and heavy rare earth elements (HREE), including Gd, Tb, Dy, Ho, Er, Tm, Yb and Lu [12]. Also, REE may be classified as middle rare earth elements (MREE) founded on their atomic mass and effective ion radius and comprises the elements Sm, Eu, Gd and Tb [13]. REEs have significant applications in modern healthcare, telecommunication, agriculture, petroleum refining, automotive, electronic components, semiconductor and defense, etc. [5].

In Nigeria, the mining sector boasts more than 40 different types of commercially viable minerals. Only clay-rich sediments are mined in more than 80 clay deposits in all parts of the country. Examples are, clay deposits in Abak, Akwa Ibom State, Uruove near Ughelli in Delta State, Ifon in Ondo State, Mokola in Oyo State, Sokoto in Sokoto State, Gombe in Gombe State, Dangara in Niger State, Umuahia in Abia State, Onitsha in Anambra State and Kutigi in Niger State, etc [14]. During exploitation of these minerals, soil, air, and water pollution may occur especially when these operations are done in an artisanal manner as seen in most mining areas in Nigeria [15].

The main aim of this work is to investigate the REE distribution in Nigerian soil samples from a clay mining area with the goal of assessing their concentrations, distribution pattern, and possible contamination. For comparison, soil samples from a farmland, located at approximately 3 km away, out of the influence of the mining site and considered non-contaminated, was chosen as the control site. Elemental concentrations and mineralogy were determined by instrumental neutron activation analysis (INAA) and X-ray diffraction (XRD) respectively.

2. MATERIALS AND METHODS

2.1. Study Area

The study area is located in Umuahia South, Abia State, Southeast, Nigeria, where the mining of clay is being carried out. The coordinates of the sampling points are presented in supplementary material S1. Umuahia South is one of the local government areas of Abia State and the sampling location is shown in Figure 1. It has a mean area of 140 km² and a population of 138,570 according to the 2006 census. For comparison, four points were chosen as a control area in farming land and a built-up area, about 3 km from the clay mining site.

The mining site is about 5 km from Umuahia town and about 30 km from Aba, Enyimba City of Abia state. The most common occupation of Umuahia is trading and some are civil servants. The average annual temperature is 26.4°C. About 2333 mm of precipitation falls annually. The vegetation is ordinarily considered part of tropical rain forest which is the dominant natural vegetation in most parts of southern Nigeria.

Figure 1: Location of Umuahia south, Aba express road, Abia state, Nigeria

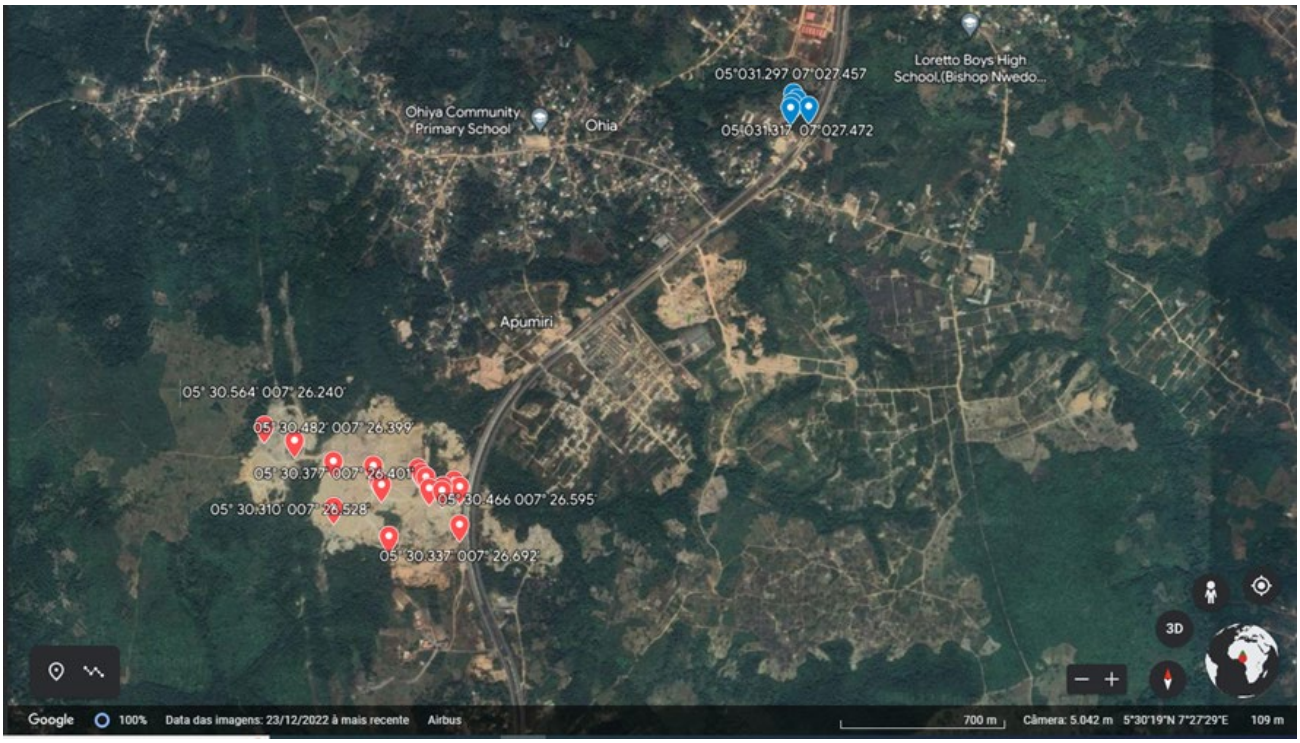

2.2. Samples Preparation

Soil samples were collected randomly covering the entire mining sites. All the soil samples were collected using an auger sampler at a depth of 5-15 cm for every sampling point, and the soil samples were lowered into the labeled plastic bags [16]. At each point, about 1 to 1.5 kg was collected. Every bag with a soil sample was properly sealed and then transported to the laboratory for preparation processes.

At the laboratory, the soil samples were air dried in trays for 7 days and then oven dried at a temperature of 105°C for between 3-4 hours until they presented a constant weight [17], at the central laboratory of Federal University Wukari. After drying the soil samples were pounded using a mortar and pestle. A sieve of mesh size 2 mm recommended in [18] was used to obtain uniform particle sizes. The sieved prepared soil samples were flown to Nuclear and Energy Research Institute (IPEN from the Portuguese Instituto de Pesquisas Energéticas e Nucleares) São Paulo, Brazil, for analysis. At IPEN, approximately 80 mg and 120 mg of reference materials (Syenite, Table Mountain, STM-2 from USGS and Standard Reference Material SRM-1646a from NIST) and samples were prepared and weighed for irradiation. Each of the samples and reference materials were tightly sealed in clean polyethylene bags, to avoid contamination. Chemical standard solutions were also prepared, pipetted in filter paper strips.

2.3. Analysis of Samples

The samples, reference materials and pipetted samples were placed in separated polyethylene and wrapped in aluminum foils, packaged in aluminum containers, named rabbits, and hermetically sealed for irradiation. In the irradiation scheme, samples were irradiated for 8 hours and allowed to decay for seven days before the first counting set, and for 15 days for the second counting set. Samples, reference materials and pipetted standards were counted for 7200 seconds.

For the gamma counting a p-types high pure germanium detector (HPGe), from Canberra (USA), with relative efficiency ≥ 40%, resolution ≤ 1.800 keV FWHM at 1.33 MeV was used. Daily verification performance was done using the isotopes ^{57}Co, with an energy of 122 keV and ^{60}Co with an energy of 1332 keV. The data analysis was done using the stationary in house gamma ray software programme known as CAX, which identifies the required gamma ray peaks of the interested nuclide elements [19].

For X-Ray diffraction analysis, a SmartLab SE diffractometer from Rigaku was used with a Cu Tube X-Ray generator (λ=1.54Å). The measurements were performed in powder samples in a range from 10º to 70º at a speed of 1º/min and step of 0.02º.

2.4. Geo-accumulation Index (IGeo)

Geo-accumulation index is applied in the determination of the extent of anthropogenic influence and compares various metals existing in the earth's crust [20]. It was first applied by [21] and has been used by many authors. Mathematically, it can be computed using Equation 1:

$$Igeo = C_{REE}/(1.5B_n) \quad (1)$$

Where IGeo is the geoaccumulation index, C_{REE} is the concentration of the REE in the material soil sample (μg g^{-1}), B_n is the concentration of the REE in control or reference value (μg g^{-1}), and the factor 1.5 is employed to reduce the possible variations in the background data because of lithological variations in material sample concentration. Lithological variation is the natural factor that affects the spatial elemental distribution in the soil [22]. The following are the range of categories of the geo-accumulation index [23].

IGeo ≤ 0 (not contaminated)

0 ≤ IGeo ≤1 (not contaminated to moderately contaminated)

1 ≤ IGeo ≤2 (moderately contaminated)

2 ≤ IGeo ≤3 (moderately to heavily contaminated)

3 ≤ IGeo ≤4 (severely contaminated)

5 ≤ IGeo ≤5 (severely to extremely contaminated)

IGeo > 5 (extremely contaminated)

The upper continental crust (UCC) REE concentrations were applied for values of Bn.

3. RESULTS AND DISCUSSIONS

The mineralogical characterization of the soil samples from the clay mining area and from the control site are depicted in the diffractograms shown in Figures 2 and 3. The samples from both sites are basically composed of silicates and kaolinite. The reference crystallographic files (ICSD database) are positioned below the experimental fractograms and are identified by their reference numbers.

Figure 2: Diffractogram of soil samples from the clay mining area

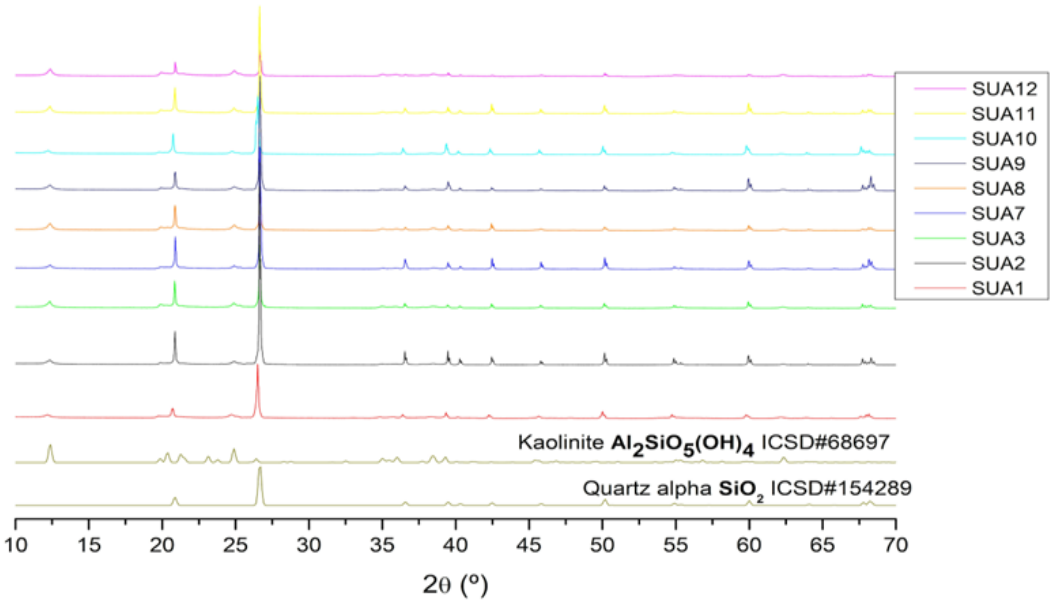

Figure 3: Diffractogram of one soil sample from the control area

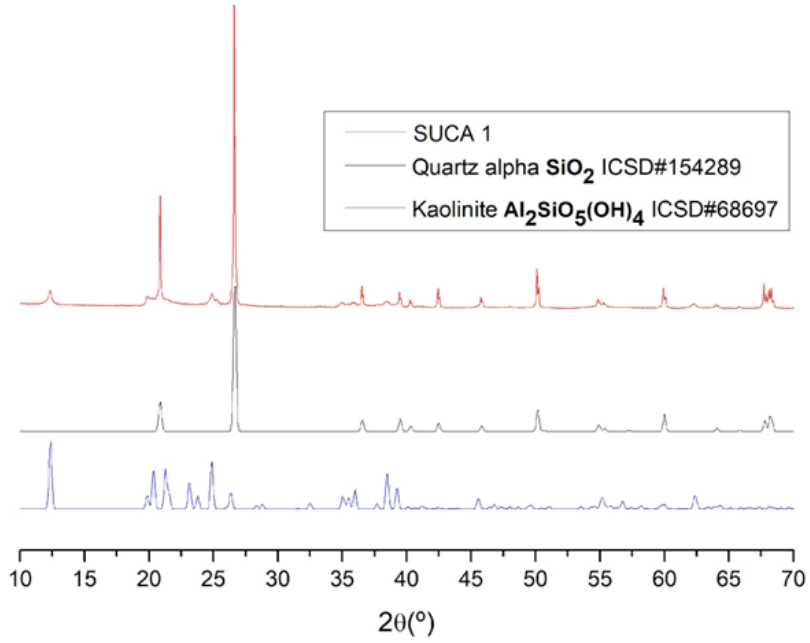

Table 1 depicts the results of REE concentration of the samples collected in the clay mining site and the concentrations of the samples collected in the control area. For comparison it was also added the REE concentrations of UCC and for the North American Shale Composite (NASC). In Figure 4 it is presented the logarithmic distribution pattern of the samples (SUA), control (SUCA) and UCC and NASC for comparison.

It can be seen in Figure 4 that no significant difference exists between samples from the clay site mining, control site, UCC and NASC indicating that the REE present in the samples are of natural origin. This conclusion is corroborated by the IGeo values shown in Table 2, where it can be seen that, with just a few exceptions, the values are < 0. Only the samples SUA3 and SUA7 presented Igeo values > 1 for Lu and SUCA2 for Ce. As no evidence of a pollution source could be identified, these values may probably be attributed to a variation in soil matrix, such as organic matter, changes in pH and redox potential [24]. The REE concentrations found are in good agreement with those found by [25] for soils from Nigerian semi-savanna and rain forest regions.

Figure 4: Distribution pattern comparing the REE concentrations, for the samples (SUA), control (SUCA), UCC and NASC. Summation of the rare earth elements (ΣREE), summation of the light REE (ΣLREE) and summation of the heavy REE (ΣHREE)

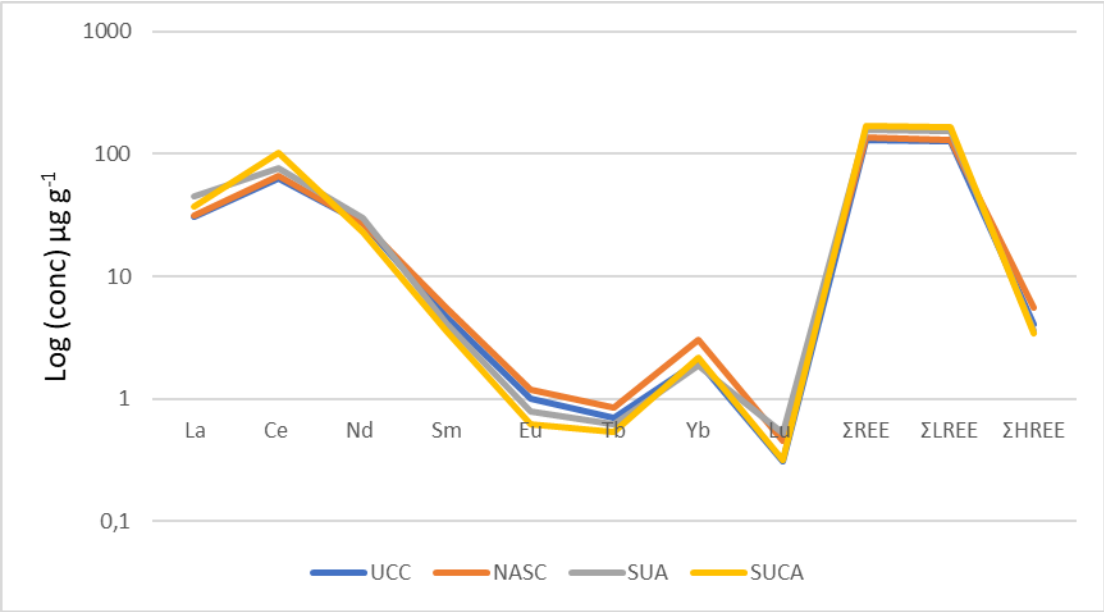

In Figures 5 and 6, the normalized REE by UCC and chondrite, respectively, are shown. For comparison, the normalized summation of ∑REE, ∑LREE and ∑HREE are also presented.

The normalization using UCC indicates that a fractionation has occurred between light and heavy rare earth elements in these soil samples. Higher values of fractionation occur for Ce in one sample (SUCA2), from the control area, and for Lu, in five samples (SUA3, SUA5, SUA7, SUA16 and SUA17) with no clear pattern between them for this element. For the normalization made with the chondrite, two samples present a divergent behavior for Ce (SUA12 and SUCA2). Cerium anomaly, denoted by Ce*, may occur in an oxidant environment when Ce(III) is oxidized to the more insoluble Ce(IV). Considering the used equation for Ce* calculation, Ce anomaly values may be negative (< 0), i.e., Ce depletion relative to neighboring REE (normalized to chondrite or shale) or present positive (> 0) values indicating Ce enrichment [26]. Europium anomaly, denoted by Eu*, may also occur.

If Eu has been present exclusively as Eu(III) it will behave as its closest lanthanides neighbors.

Table 1: Concentrations, in μg g^{-1}, of the REE in the samples from the clay mining area (SUA) and from the control site (SUCA), upper continental crust (UCC), chondrite and North American Shale Composite (NASC)

	La	Ce	Nd	Sm	Eu	Tb	Yb	Lu
SUA	64. ± 0.	58 ± 3	38 ± 5	6.6 ± 0.	0.8 ± 0.	0.5 ± 0.	2.3 ± 0.	0.1 ± 0.0
SUA	26. ± 0.	56 ± 2	21 ± 2	2.3 ± 0.	0.8 ± 0.	N	0.9 ± 0.	0.1 ± 0.0
SUA	70 ± 2	12 ± 3	42 ± 7	6.0 ± 0.	N	0.7 ± 0.	2.6 ± 0.	1.4 ± 0.0
SUA	67 ± 1	11 ± 2	33 ± 6	4.8 ± 0.	N	0.5 ± 0.	2.7 ± 0.	N
SUA	43 ± 1	60. ± 0.	33 ± 6	3.2 ± 0.	0.7 ± 0.	0.4 ± 0.	2.0 ± 0.	0.8 ± 0.0
SUA	60 ± 2	56. ± 0.	37 ± 5	5.3 ± 0.	0.8 ± 0.	0.5 ± 0.	2.6 ± 0.	0.3 ± 0.0
SUA	66 ± 2	11 ± 3	35 ± 8	6.9 ± 0.	1.2 ± 0.	0.7 ± 0.	2.0 ± 0.	1.2 ± 0.0
SUA	39 ± 1	79 ± 4	29 ± 3	2.8 ± 0.	0.5 ± 0.	N	1.1 ± 0.	0.2 ± 0.0
SUA	45. ± 0.	82 ± 2	31 ± 3	3.9 ± 0.	0.5 ± 0.	0.5 ± 0.	1.6 ± 0.	0.2 ± 0.0
SUA	30 ± 1	42 ± 1	30 ± 3	3.4 ± 0.	0.6 ± 0.	0.9 ± 0.	1.5 ± 0.	0.2 ± 0.0
SUA	47. ± 0.	65 ± 1	31 ± 4	4.4 ± 0.	0.7 ± 0.	0.9 ± 0.	1.2 ± 0.	0.2 ± 0.0
SUA	35. ± 0.	14 ± 3	N	2.3 ± 0.	0.9 ± 0.	0.6 ± 0.	1.6 ± 0.	0.2 ± 0.0
SUA	28 ± 1	43 ± 1	18 ± 4	2.3 ± 0.	0.4 ± 0.	0.2 ± 0.	1.5 ± 0.	0.5 ± 0.0
SUA	28. ± 0.	52 ± 1	15 ± 3	3.0 ± 0.	0.4 ± 0.	N	1.4 ± 0.	0.3 ± 0.0
SUA	47 ± 1	95 ± 5	36 ± 4	5.3 ± 0.	1.3 ± 0.	0.7 ± 0.	2.5 ± 0.	0.6 ± 0.0
SUA	45 ± 1	91 ± 2	35 ± 2	5.3 ± 0.	1.3 ± 0.	0.8 ± 0.	2.4 ± 0.	0.6 ± 0.0
SUA	26. ± 0.	43 ± 1	15 ± 4	2.3 ± 0.	0.4 ± 0.	0.2 ± 0.	1.5 ± 0.	0.5 ± 0.0
SUC	37. ± 0.	64 ± 3	24 ± 2	3.7 ± 0.	0.5 ± 0.	0.5 ± 0.	2.3 ± 0.	0.3 ± 0.0
SUC	37. ± 0.	23 ± 8	22 ± 2	4.1 ± 0.	±	0.4 ± 0.	1.8 ± 0.	±
SUC	43. ± 0.	69 ± 2	29 ± 1	3.7 ± 0.	0.7 ± 0.	0.7 ± 0.	2.8 ± 0.	0.3 ± 0.0
SUC	31. ± 0.	49 ± 2	17 ± 1	2.9 ± 0.	0.5 ± 0.	0.4 ± 0.	1.9 ± 0.	0.3 ± 0.0
UCC	31	63	27	4.7	1	0.7	2	0.3
Chon	0.2	0.6	0.4	0.1	0.0	0.0	0.1	0.0
NAS	31.	66.	27.	5.5	1.1	0.8	3.0	0.4

Conversely, if Eu is present in its reduced form, as Eu(II), this result is the so-called Eu anomaly [27]. According to the used equation, positive Eu* will present values higher than 1 and negative Eu* will present values lower than 1.

Table 2: IGeo values calculated for the samples from the clay mining area (SUA) and from control area (SUCA)

	La	**Ce**	**Nd**	**Sm**	**Eu**	**Tb**	**Yb**	**Lu**
SUA 1	0.48	-0.72	-0.08	-0.11	-0.90	-0.84	-0.40	-1.50
SUA 2	-0.82	-0.75	-0.96	-1.61	-0.90	ND	-1.67	-1.50
SUA 3	0.60	0.39	0.06	-0.22	ND	-0.54	-0.20	1.64
SUA 4	0.53	ND	-0.28	-0.55	ND	-0.94	-0.14	ND
SUA 5	-0.12	-0.66	-0.29	-1.12	-0.92	-1.25	-0.58	0.93
SUA 6	0.36	-0.75	-0.14	-0.40	-0.84	-0.85	-0.21	-0.29
SUA 7	0.50	0.31	-0.22	-0.03	-0.22	-0.43	-0.54	1.37
SUA 8	-0.27	-0.26	-0.48	-1.31	-1.38	ND	-1.48	-0.73
SUA 9	-0.02	-0.20	-0.40	-0.84	-1.44	-1.04	-0.87	-0.93
SUA 10	-0.65	-1.18	-0.45	-1.04	-1.33	-0.09	-0.96	-0.96
SUA 11	0.04	-0.53	-0.37	-0.68	-1.09	-0.23	-1.30	-0.70
SUA 12	-0.37	0.58	ND	-1.59	-0.71	-0.70	-0.89	-0.86
SUA 13	-0.76	-1.13	-1.14	-1.61	-1.88	-2.03	-0.96	0.29
SUA 14	-0.73	-0.85	-1.42	ND	-1.77	ND	-1.08	-0.38
SUA 15	0.02	0.01	-0.15	-0.41	-0.21	-0.51	-0.24	0.50
SUA 16	-0.05	-0.05	-0.21	-0.40	-0.20	-0.37	-0.35	0.51
SUA 17	-0.83	-1.12	-1.41	-1.61	-1.88	-2.02	-0.95	0.30
SUCA 1	-0.31	-0.56	-0.78	-0.95	-1.35	-0.98	-0.41	-0.61
SUCA 2	-0.31	1.29	-0.86	-0.77	ND	-1.22	-0.71	ND
SUCA 3	-0.09	-0.45	-0.46	-0.91	-1.09	-0.52	-0.11	-0.45
SUCA 4	-0.56	-0.95	-1.25	-1.28	-1.45	-1.31	-0.67	-0.62

ND – not determined.

These changes in redox conditions may the responsible for the higher observed Ce values normalized by the chondrite in the above-mentioned samples, since oxidizing conditions favors the tetravalent and more insoluble Ce form. No significant fractionation was observed for Eu in the samples.

The values for Ce* and Eu* anomaly is presented in Table 3. Sample SUCA2 is the one with the higher values for Ce*, and SUA12 is the one that present the highest Eu* value. Also in Table 3, the values of the La_N/Yb_N, La_N/Lu_N, La_N/Lu_N, ∑REE, ∑LREE, ∑HREE, and $\sum LREE_N/\sum HREE_N$ are shown. The ∑REE varied from 89.85 to 246.99, with a mean value of 158.67 μg g^{-1}, very similar to this values when calculated for UCC and NASC. Except for the samples SUCA2, the $\sum LREE_N/\sum HREE_N$ are very close to the unity in the control site, while the samples of the clay mining area generally present values slightly higher. The high value of this ratio may arise out of the higher affinity of LREEs for the clay fraction in the soil system [28].

Figure 5: Normalized REE from clay mining and control areas by upper continental crust (UCC)

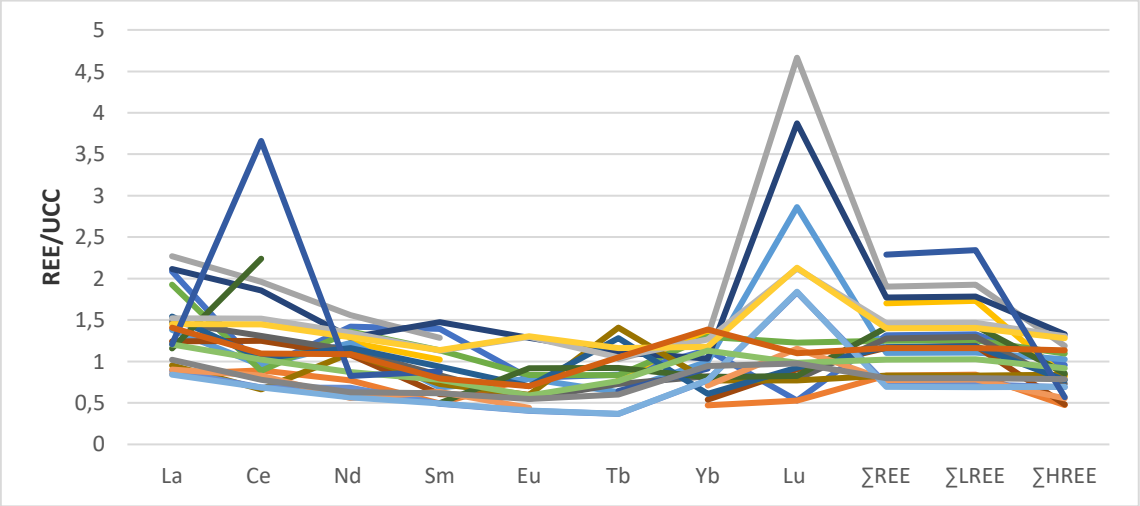

Figure 6: Normalized REE from clay mining and control areas by chondrite

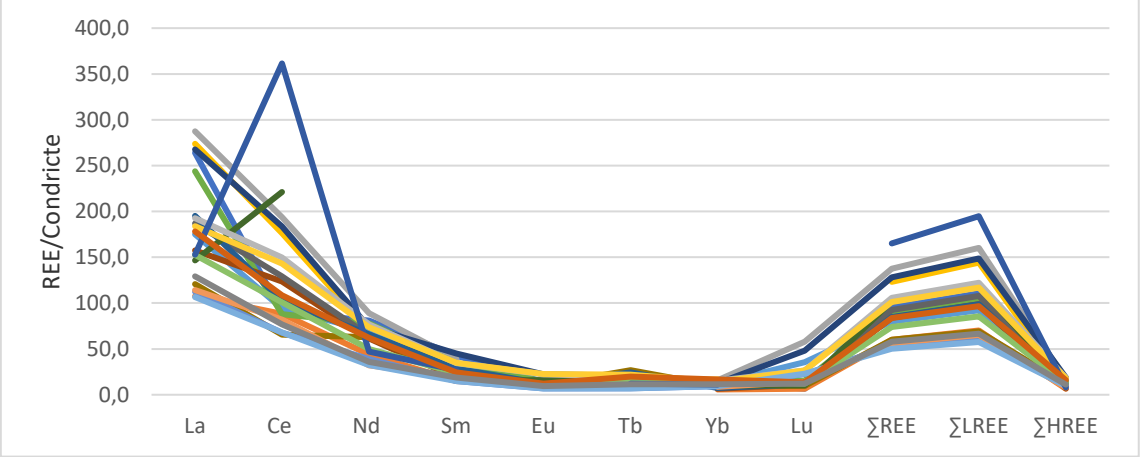

In the attempt to characterize the clay samples according to their REE pattern, principal component and classification analysis was applied. The result is shown in Figure 7. The samples with positive loading for the first and second factors are characterized by the higher values of the ∑REE, ∑LREE, and $\sum LREE_N/\sum HREE_N$ ratio. This factor also includes sample SUCA2 that present a high Ce* value. Samples with positive loading for the first factor and negative loadings for the second factor (fourth quadrant) are characterized by the higher values of La_N/Yb_N, La_N/Lu_N, La_N/Lu_N ratios.

Table 3: Normalization values of the REE in the soil samples from the clay mining and control area

	Ce*	Eu*	La_N/Yb_N	La_N/Lu_N	Sm_N/Yb_N	∑REE	∑LREE	∑HREE	$\sum LREE_N/\sum HREE_N$
SUA 1	-0.50	0.68	19.11	3.94	1.22	170.95	167.12	3.83	1.39
SUA 2	0.09	ND	18.81	1.60	1.05	107.61	105.70	1.91	1.77
SUA 3	-0.02	ND	18.19	0.49	0.99	246.99	242.22	4.77	1.62
SUA 4	-1.00	ND	16.56	ND	0.75	221.00	217.72	3.28	2.12
SUA 5	-0.28	1.18	14.44	0.48	0.69	143.31	139.19	4.12	1.08
SUA 6	-0.48	0.82	15.52	1.57	0.87	162.29	157.90	4.40	1.15
SUA 7	0.04	0.96	21.34	0.55	1.42	229.75	224.42	5.33	1.34
SUA 8	0.05	ND	24.10	1.37	1.12	151.22	149.29	1.93	2.46
SUA 9	-0.03	0.69	18.78	1.87	1.02	165.77	162.82	2.95	1.76
SUA 10	-0.34	0.66	12.91	1.24	0.95	107.79	104.42	3.37	0.99
SUA 11	-0.26	0.68	26.41	1.67	1.54	152.05	148.94	3.11	1.53
SUA 12	ND	1.50	14.90	1.40	0.61	182.79	179.35	3.44	1.66
SUA 13	-0.16	0.91	12.01	0.48	0.64	94.19	91.41	2.78	1.05
SUA 14	0.08	ND	13.24	0.78	0.89	100.58	98.36	2.22	1.41
SUA 15	0.04	1.18	12.54	0.72	0.89	189.60	184.37	5.23	1.13
SUA 16	0.04	1.14	12.87	0.68	0.97	181.70	176.56	5.14	1.10
SUA 17	-0.07	0.91	11.35	0.46	0.64	89.85	87.06	2.79	1.00
SUCA 1	-0.06	0.76	11.14	1.23	0.69	132.59	128.90	3.69	1.11
SUCA 2	2.44	ND	13.77	ND	0.96	296.81	294.52	2.28	4.12
SUCA 3	-0.15	0.80	10.61	1.28	0.58	150.52	145.97	4.55	1.02
SUCA 4	-0.10	0.90	11.27	1.05	0.65	103.73	100.57	3.16	1.01

ND – not determined.

The subscript N indicates that the concentration is normalized by the UCC. Ce* was calculated by the formula $Ce^*/Ce_N = ((La/La_N)^{2/3} \times (Nd/Nd_N)^{1/3}) - 1$[29]. Eu* was calculated by the formula $Eu^* = Eu_N/(Sm_N^2 \times Tb_N)^{1/3}$ [26].

All the other samples compose a more homogeneous group. The samples presenting enrichment in LREE are probably related to the amount of kaolinite that is a detrital mineral, generally derived from highly weathered soils [30], since REE may be adsorbed as impurities or incorporated as substituting elements into the crystalline structure of this host minerals [31].

Figure 7: Principal component and classification analysis obtained for the soil samples from the clay mining and control area based in the data presented in Table 3

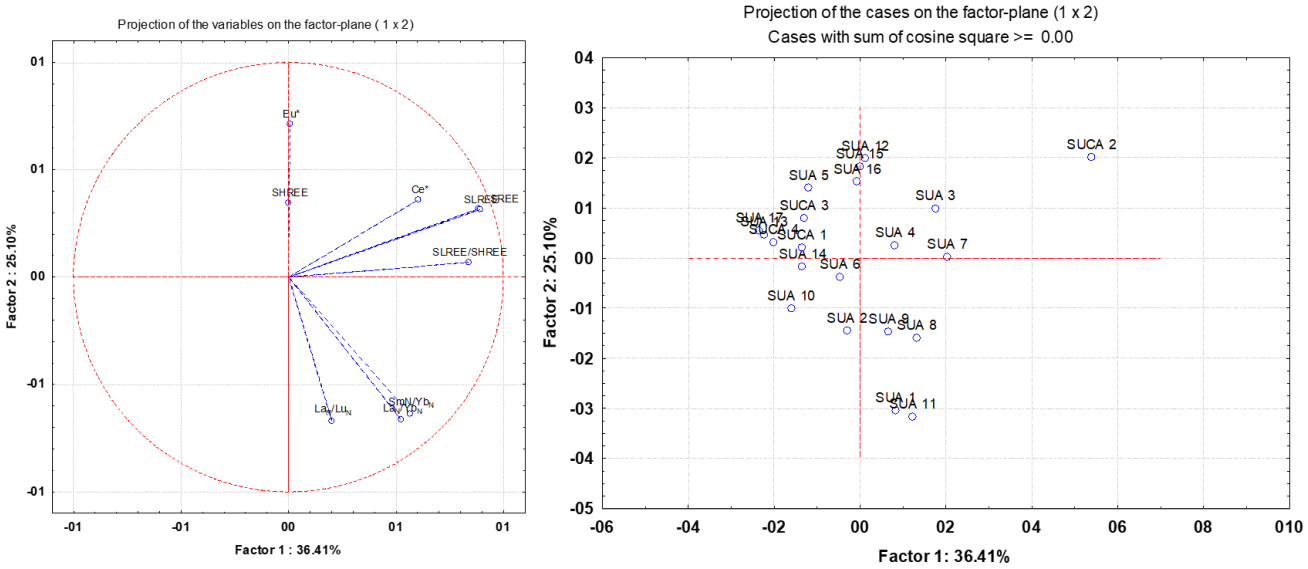

4. CONCLUSIONS

The samples of soil collected in a clay mining area, from Umuahia, Abia Stae, Southeast, Nigeria, as well as, soil samples from an area chosen as control, approximately 3 km away, from a farmland area, was analyzed to determine the REE concentration, their distribution pattern, mineralogy and possible anthropogenic contamination.

It was determined that the soil samples are composed basically of silicate and kaolinite minerals. The obtained concentrations are in agreement with the ∑REE of 130 μg g^{-1} to 240 μg g^{-1} and comparable with the global standards UCC and NASC. IGeo values, calculated using the UCC values as normalizer indicate that no anthropogenic influence can be observed in these samples, being the incorporation of the REE in the soil samples a result of geological

processes probably related to the weathering process that control the soil formation. An enrichment of LREE was observed over the HREE, mainly in the samples from the clay mining area. This enrichment should be linked to the fact that LREE are more easily bound to the clay fraction of the soil.

CONFLICT OF INTEREST

The authors declare that they have no competing financial interests or personal relationships that may have influenced the work reported in this study.

REFERENCES

[1] SANTANA, M. L. T.; CARVALHO, K. M.; PEIXOTO, A. U. S.; JUNIOR CESAR, M. E.; VAN ES, H. M., CURI, N.; MONTOANI, B. Interactions between Land Use and Soil Type Drive Soil Functions, Highlighting Water Recharge Potential, in the Cantareira System, Southeast of Brazil. **Sci Total Environ**, v. 903, p. 166125, 2023.

[2] MULYONO, A.; SETIAWAN, I.; HIDAYAT, E.; NOVIARDI, R. 'Distribution and Potential Contamination Assessment of Rare Earth Elements (REE) in Indonesian Volcanic Soil'. **Acta Ecol Sin**, p. 1-10, 2023.

[3] Oladipo, H. J., Tajudeen, Y. A.; Taiwo, E. O.; Muili, A. O.; Yusuf, R. O.; Jimoh, S. A.; Oladipo, M. K.; Oladunjoye, I. O.; Egbewande, O. M.; Sodiq, Y. I.; Ahmed, A. F.; El-Sherbini, M. S. 'Global Environmental Health Impacts of Rare Earth Metals: Insights for Research and Policy Making in Africa'. **Challenges, v.** 14(20), p. 1-13, 2023.

[4] ILEVBARE, M. 'Rare Earth Elements of Ajali Sandstone, SW, Anambra Basin in Nigeria: Implication for Soil Genesis'. **J Appl Sci Environ Manag**, v. 24(11), p. 1999–2004, 2021.

[5] MALHOTRA, N.; HSU, H. S.; LIANG, S. T.; ROLDAN, M. J. M.; LEE, J. S.; GER, T. R.; HSIAO, C. D. An Updated Review of Toxicity Effect of the Rare Earth Elements (REEs) on Aquatic Organisms'. **Animals,** v. 10(9), p. 1–27, 2020.

[6] HAQUE, N.; HUGHES, A.; LIM, S.; VERNON, C. Rare Earth Elements: Overview of Mining, Mineralogy, Uses, Sustainability and Environmental Impact. **Resources,** v. 3(4), p. 614–35, 2014.

[7] SOLTANI, F.; ABDOLLAHY, M.; PETERSEN, J.; RAM, R.; KOLEINI, S. M. J.; MORADKHANI, D. Leaching and Recovery of Phosphate and Rare Earth Elements from an Iron-Rich Fluorapatite Concentrate: Part II: Selective Leaching of Calcium and Phosphate and Acid Baking of the Residue'. **Hydrometallurgy**, v 184, p. 29–38, 2019.

[8] ZEPF, V. Rare Earth Elements: What and Where They Are. In: Rare Earth Elements. Springer Theses. Springer, Berlin, Heidelberg, p 11–39, 2013.

[9] PAGANO, G.; THOMAS, P. J.; NUNZIO, A.; TRIFUOGGI, M. Human Exposures to Rare Earth Elements: Present Knowledge and Research Prospects. **Environ Res**, v. 171, p. 493–500, 2019.

[10] ELIAS, M. S., AZMAN, M. A.; DAUNG, J. A. D.; HASHIM, A.; LAILI, Z.; OMAR, S. A.; SHUKOR. S. Assessment of Rare Earth and Actinides (U and Th) Elements in Soil Samples from Kapar Industrial Area, Selangor'. **IOP Conf Ser: Mater Sci Eng**, **v.** 1231(1), p. 1-12, 2022.

[11] KHADHAR, S.; SDIRI, A.; CHEKIRBEN, A.; AZOUZI, R.; CHAREF, A. Integration of Sequential Extraction, Chemical Analysis and Statistical Tools for the Availability Risk Assessment of Heavy Metals in Sludge Amended Soils. **Environ Pollut**, v. 263, p. 114543, 2020.

[12] OMODARA, L.; PITKÄAHO, S.; TURPEINEN, E.; SAAVALAINEN, P.; ORAVISJÄRVI, K.; KEISKI, R. L. Recycling and Substitution of Light Rare Earth Elements, Cerium, Lanthanum, Neodymium, and Praseodymium from End-of-Life Applications - A Review. **J Clean Prod,** v. 236, p. 117573, 2019.

[13] ARRACHART, G.; COUTURIER, J.; DOURDAIN, S.; LEVARD, C.; PELLET-ROSTAING, S. 'Recovery of Rare Earth Elements (REEs) Using Ionic Solvents'. **Processes**, v. 9(7), p. 1202, 2021.

[14] ODOMA, A. N., OBAJE, N. G.; OMADA, J. I.; IDAKWO, S. O.; ERBACHER, J. Mineralogical, Chemical Composition and Distribution of Rare Earth Elements in Clay-Rich Sediments from Southeastern Nigeria. **J African Earth Sci,** v.102, p. 50–60, 2015.

[15] KASIMBAZI, E. Chapter 31: Regulating Environmental Impacts Associated with Mining in Uganda. in **Law | Environment | Africa**., p. 665–96, 2019.

[16] FAANU, A.; EPHRAIM, J. H.; DARKO, E. O. Assessment of Public Exposure to Naturally Occurring Radioactive Materials from Mining and Mineral Processing Activities of Tarkwa Goldmine in Ghana'. **Environ Monit Assess**, v. 180(1–4), p. 15–29, 2011.

[17] IAEA, INTERNATIONAL ATOMIC ENERGY AGENCY. **Measurement of Radionuclides in Food and the Environment** - Technical Reports Series No. 295, 1989.

[18] IAEA, INTERNATIONAL ATOMIC ENERGY AGENCY. **Extent of Environmental Contamination by Naturally Occurring Radioactive Material (NORM) and Technological Options for Mitigation**, Technical Reports Series No. 41, 2003.

[19] ZAHN, G. S.; JUNQUEIRA, L. S.; GENEZINI, F. A. CAX and Xsel: A Software Bundle to Aid in Automating NAA Spectrum Analysis. **Braz J Radiat Sci**, 7(2A).

[20] JENA, V.; GHOSH, S.; PANDE, A.; MALDINI, K.; MATIC, N. 2019. Geo-Accumulation Index of Heavy Metals in Pond Water Sediment of Raipur. **Biosci Biotechnol Res Commun,** v. 12(3), p. 733–36, 2019.

[21] MULLER, G. 'Index of Geoaccumulation in Sediments of the Rhine River'. **GeoJournal** v. 2, p. 108 – 18, 1969.

[22] TIMOTHY, M. N.; MARCUS, A. C.; IYAMA, W. A. Assessment of Trace Metal Content in Soils of Automobile Workshops around Bori Urban Area, Rivers State, Nigeria. **Eur j appl sci**, v. 10(3), p. 209 – 221, 2022.

[23] ALGÜL, F; BEYHAN. M. Concentrations and Sources of Heavy Metals in Shallow Sediments in Lake Bafa, Turkey'. **Sci Rep**, v. 10(1), p.11782, 2020.

[24] LIN, R., BANK, T. L., ROTH, E. A., GRANITE, E. J., SOONG, Y. Organic and inorganic associations of rare earth elements in central Appalachian coal, **Int J Coal Geol**, v. 179, p. 295-301, 2017.

[25] IMASUEN, O. I.; FYFE, W. S.; OLORUNFEMI, B. N.; ASUEN, G. O.; Zonal Mineralogical/Geochemical Characteristics of Soils of Midwestern Nigeria." **J African Earth Sci**, v. 8(1), p. 41–49, 1989.

[26] ZHANG, K.; SHIELDS, G. A. "Early Diagenetic Mobilization of Rare Earth Elements and Implications for the Ce Anomaly as a Redox Proxy. **Chem Geol**, v. 635, p. 121619, 2023.

[27] LIDMAN, F., LAUDON, H.; TABERMAN, I.; KÖHLER, S. Eu Anomalies in Soils and Soil Water from a Boreal Hillslope Transect – A Tracer for Holocene Lanthanide Transport? **Geochim Cosmochim Acta,** v. 267, p.147–63, 2019.

[28] HENDERSON, P. **Rare Earth Element Geochemistry**. Rare Earth Element Geochemistry. 2nd ed. London, 1983.

[29] BARRAT, J. A., BAYON, G.; LALONDE. S. Calculation of Cerium and Lanthanum Anomalies in Geological and Environmental Samples. **Chem Geol**, v. 615, p. 121202, 2023.

[30] ANDRADE, G. R. P.; JAVIER CUADROS, J. M. P. B.; VIDAL-TORRADO, P. Clay Minerals Control Rare Earth Elements (REE) Fractionation in Brazilian Mangrove Soils. **Catena,** v. 209(P2), p. 105855, 2022.

[31] GUIMAPI, N. T.; TEMATIO, P.; TIOMO, I. F.; HAPPI, F. D.; FOTSO, A. K.; TCHAPTCHET, C. W. T. "Redistribution and Fractionation of Trace and Rare Earth Elements during Weathering and Lateritization of Orthogneiss in Ndokayo (Bétaré-Oya Gold District, South East Cameroon)." **Geoderma Reg, v.** 32, p. e00601, 2023.

LICENSE